Toward efficient control of energy systems: an application of proper generalized decomposition to thermal storage

***A. Sciacovelli*[a]**

[a] *Birmingham Centre for Energy Storage, School of Chemical Engineering, University of Birmingham, UK, a.sciacovelli@bham.ac.uk*

Abstract:

The need of sustainable use of available energy resources is undeniable. This can be achieved only through 1) efficient *design* of energy systems and 2) optimal *control* of energy systems during operation. Traditionally, these two tasks are tackled with opposite modeling strategies. Complex and computationally expensive models (CFD, finite elements, etc.) are used for designing purposes; simplified inexpensive models (black box models, transfer functions, etc.) are employed for control purposes.

In this paper we consider and alternative approach called Proper Generalized Decomposition (PGD) that combines the accuracy of CFD with the "lightness" of black box models. A thermocline thermal energy storage (TES) system is considered in the present analysis to show the attractive features of PGD. An accurate but at the same time computationally inexpensive model is developed considering a solution in a separate form (i.e. a PGD solution) of the energy equation which describes the evolution of the TES temperature both in time and space. More thrillingly, we show how to include *a priori* in the solution the effect of design/operational parameters by finding once for all a generalized solution which, beside space and time, contains the parameters as further "dimensions".

To summarize, this work presents a novel approach to energy systems modeling which combines both accuracy, computational efficiency, and flexibility. These features makes PGD an attractive methodology which is worth of further use in the field of energy systems design and control.

Keywords:

Thermal energy storage; Proper generalized decomposition; Model order reduction; Control.

1. Introduction

1.1 – Energy systems modeling: current paradigm

A model, as defined by the philosopher Ludovico Geymonat (1908-1991) [1], is a quantitative description of a real phenomenon (or system), obtained from the application of theories, that are built to obtain information on the phenomenon (or system). The need of modeling arises from a question that is posed concerning the phenomenon/system which cannot be answered directly. The same inquiry is posed to the model which answer becomes the reply to the question on the phenomenon/system. Since the dawn of scientific method, models have been persistently developed by researchers to acquire insight into physical phenomena and to develop new technologies. Nowadays, modern engineering strongly relies on modeling in order to deal with complex problems. The complexity may arise from intricate physical phenomena, unconventional geometry of systems, variable operating conditions, uncertainties, etc. Nevertheless, when a model is built the ultimate goal consists in developing the most simple model possible, but still able to characterize the physical phenomena involved in the problem. In a nutshell, referring to a quote attributed to A. Einstein, "[a model] should be as simple as possible but not simpler". This translates to the necessity of models that predict *quickly* and *accurately* the behaviour of *complex* engineering systems. Up to now, fast and accurate solutions of complex models are usually achieved at the expense of high computational efforts by means of high performance computational platforms.

Such a drawback is particularly relevant in the field of energy systems modeling. In particular, we can identify three challenging scenarios associated with modeling of energy systems:

- *Performance prediction*. This represents the most straightforward modeling approach; it consists in using models to quantify the performance of the energy systems. Frequently, performance prediction is carried out to test novel configurations (i.e. prototypes) of the studied system before their actual fabrication. Established modeling strategies for performance predictions are black box models [2] and computational fluid dynamic (CFD) models [2,3]. In addition, also models at the molecular level [4] have been more frequently used in the last years. In the framework of performance prediction modeling challenges stem from the multiphysics, multiscale and coupled phenomena involved in advanced energy systems. This results in non-linear models with a fine resolution of both space and time scales leading to a severe computational burden (i.e. high computational costs).
- *Design optimization*. In the area of energy systems a central task consists in devising systems which accomplish a stated goal in the best possible way. In other terms, the design of optimal systems. Traditionally, design optimization is performed through a combined use of parametric modeling and optimization algorithms [5]. In principle, each feasible design, identified by a specified set of parameters (i.e. design variables), has to be evaluated to find the optimal one. This requires the direct computation of a solution of the associated model for each possible combination of the values of the design variables. Although optimization algorithms facilitate such a search, this traditional approach becomes soon inapplicable as model complexity and number of parameters increases. For such a reason optimizations are commonly performed using black box models [2,5], which ease the computational cost but lack of accuracy.
- *Control and optimal operation*. Once an energy system has been design it is necessary to operate it in the best possible way. Namely, the system should be controlled in such a way that optimal performance are achieved for the entire spectrum of operating condition it may face. Fast computations are a necessity in the field of modeling for control purposes. In fact, predictions by modeling should be achieved in real-time to account variable, often off-design conditions that the systems may encounter. In such a framework, black box models and transfer function are the established approaches to modeling for control purposes. Such goal oriented models achieve good computational performances at the expense of accuracy. In fact black box models and transfer function commonly steam from over simplified physics or phenomenological approaches. Thus, they often fail when used outside the framework that served to derive them.

While the previous list is far from being exhaustive, it illustrates that challenges in modeling energy systems are characterized by the lack of methods that combine accuracy, fast computation, and flexibility in the same framework. In this work we present an application of proper generalized decomposition (PGD) [6,7] for the analysis of a sensible thermal energy storage system. The analysis is aimed to show the great potentiality of PGD as a model-order reduction technique. Furthermore, we illustrate how PGD allows to account the design parameters *a-priori* in a generalized solution. These feature of PGD make it an ideal method for both design optimization and control purposes. In the next section a brief overview of fast computation methods is presented introducing model order reduction (MOR) techniques to which PGD belongs to.

1.2 – Model order reduction for fast computations

Fast calculation methods have been developed by humans throughout the ages. The period around 2700 B.C. saw the first use of the abacus, a counting frame used my merchants to facilitate quick calculations according their sexagesimal number system [8]. Subsequently, abaci appeared in various other civilizations to help in performing arithmetic calculation. Soon other forms of

"computational devices" for quick and flexible calculations appeared in the hands of engineers. Charts and nomogram are examples of such devices. They represents mathematical relations, or broadly speaking solutions for a given model, in a graphical way, enabling engineers fast calculations.

Fig. 1. Image reduction (i.e. compression) by POD. a) original image, b) contains 3% of original image, c) contains 10% of information of the original image.

Model order reduction represents a modern approach for developing simple, i.e. inexpensive, mathematical models. The ultimate goal of MOR is to reduce the complexity of dynamical models, while preserving the dynamical behaviour as much as possible [9]. Over the last three decades various MOR techniques have been developed such as, meta-models, response surface method, proper orthogonal decomposition (POD) [10]. Such methods share the common feature of extracting essential information from a pre-existing full description (i.e. a full model) of the problem under investigation. As a sequent step, the extracted information is used to reduce the full model to a compact one, that is a reduced order model. Thus, the MOR methods listed above are *a posteriori* reduction methods. As an example, Fig. 1 shows a POD reduction of the ECOS 2015 heading. It appears clear that 10% of the information contained in the original image is sufficient to identify the relevant information presented in the image.

In the next section proper generalized decomposition (PGD) is used to investigate a sensible thermal energy storage system. The analysis illustrates the attractive features of PGD: 1) the capability of performing *a-priori* model order reduction; 2) the ability of solving generalized problems which include design parameters as further dimensions beside space and time; 3) the reduced computational cost.

2. PGD for a sensible thermal energy storage system

2.1. Model reduction

Sensible thermal energy storage exploits the heat capacity of the medium to store energy in the form of sensible enthalpy. Thus, in a sensible TES energy is stored by varying the temperature of the storage medium. The latter is commonly in solid or liquid form. Common examples of storage media include water, oil, sand, rocks, and brick. The present analysis is focused on sensible TES by

liquid media. Typical application includes TES for concentrated solar power (CSP) plants, buildings, combined heat & power (CHP), and district heating networks [11]. Figure 2 shows the TES system studied in this paper. It consists in a cylindrical tank filled by the liquid storage medium. Inlet and an outlet ports allows the injection/extraction of the storage medium as the TES system is charged/discharged. The system is a so-called thermocline TES. During operation, a sharp stratification occurs in the tank due to density variation of the liquid. Hot fluid in the upper part of the tank is separated from the cold fluid by a sharp temperature gradient region commonly named thermocline. The thermocline should be confined in the smallest possible region to avoid thermal degradation, which results in lower exergetic efficiency of the TES system.

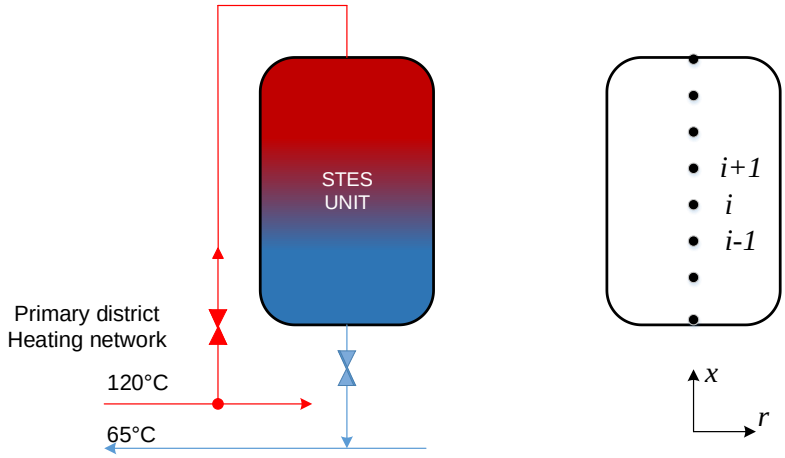

Fig. 2. Schematic of the thermal storage unit.

A one-dimensional model is here considered to describe the temperature evolution of the liquid medium in the tank. Fluid velocity is assumed uniform in the cross sectional area of the tank. Therefore, the temperature field is described by the following form of the energy equation:

$$\rho c_p \frac{\partial T}{\partial T} + \rho c_p u \frac{\partial T}{\partial x} = k \frac{\partial^2 T}{\partial x^2} \tag{1}$$

where u is the cross-section average velocity, while density, specific heat and thermal conductivity of the fluid are denoted by ρ, c_p, and k respectively. The following non-dimensional quantities

$$\hat{x} = \frac{x}{H}; \quad \hat{t} = t\frac{v}{H}; \quad \theta = \frac{T - T_{\min}}{T_{\max} - T_{\min}}$$

can be used to express Eq. (1) in its dimensionless form:

$$\frac{\partial \theta}{\partial \hat{t}} + \frac{\partial \theta}{\partial \hat{x}} = \frac{1}{\mathrm{Pe}} \frac{\partial^2 \theta}{\partial \hat{x}^2} \tag{2}$$

where $\mathrm{Pe} = uH/\alpha$ is the Peclet number.

Proper generalized decomposition aims at finding the solution of Eq. (2) in the following separated form [6]:

$$\theta(\hat{x}, \hat{t}) = \sum_{i=1}^{N} X_i(\hat{x}) C_i(\hat{t}) \tag{3}$$

Where both the number of terms N and the functions X_i, C_i are unknown so far. These are found by a progressive enrichment of the solution [6,7,12] . This means that at step n the solution is enriched adding a new contribution to the available approximated solution at step n-1, namely:

$$\theta^n(\hat{x},\hat{t}) = \theta^{n-1}(\hat{x},\hat{t}) + X_n(\hat{x})C_n(\hat{t}) = \sum_{i=1}^{n-1} X_i(\hat{x})C_i(\hat{t}) + X_n(\hat{x})C_n(\hat{t}) \tag{4}$$

The unknown functions appear in the form of a product resulting in a non-linear problem. An alternating direction strategy [6,12] is used to compute X_n and C_n. The strategy consists in two successive steps. The first step assumes $C_n(\hat{t})$ known from the previous iteration. Such know function being denoted by $S(\hat{t})$, or for simplicity S. Then, starting from S, the updated approximation $R(\hat{x})$ of the function X_n is computed. The second step of the alternating strategy consists in updating S starting from the last evaluation of R. The process continues until R converges to X_n and S to C_n. Such a strategy leads to two *separated* differential problems, as illustrated in the following:

- First step - compute $R(\hat{x})$ from $S(\hat{t})$:

At this step the solution of Eq. (2) is approximated by:

$$\theta^n = \theta^{n-1} + R(\hat{x})S(\hat{t}) \tag{5}$$

in which function S is know from the previous iteration of the alternating strategy. Using the weighted-residual form [13] of Eq. (2), i.e.

$$\int R \cdot S\left(\frac{\partial\theta}{\partial\hat{t}} + \frac{\partial\theta}{\partial\hat{x}} - \frac{1}{\mathrm{Pe}}\frac{\partial^2\theta}{\partial\hat{x}^2}\right)d\hat{x}d\hat{t} = 0 \tag{6}$$

and substituting Eq. (5) into the previous expression leads to:

$$\int R \cdot S\left(R\frac{\partial S}{\partial\hat{t}} + \frac{\partial R}{\partial\hat{x}}S - \frac{1}{\mathrm{Pe}}\frac{\partial^2 R}{\partial\hat{x}^2}S\right)d\hat{x}d\hat{t} = -\int R \cdot S\left(\frac{\partial\theta^{n-1}}{\partial\hat{t}} + \frac{\partial\theta^{n-1}}{\partial\hat{x}} - \frac{1}{\mathrm{Pe}}\frac{\partial^2\theta^{n-1}}{\partial\hat{x}^2}\right)d\hat{x}d\hat{t} \tag{7}$$

The formulation for θ^{n-1} that stems from Eq. (4) can be used to further elaborate the right-hand side of Eq. (7):

$$\begin{aligned}&\int R \cdot S\left(R\frac{\partial S}{\partial\hat{t}} + \frac{\partial R}{\partial\hat{x}}S - \frac{1}{\mathrm{Pe}}\frac{\partial^2 R}{\partial\hat{x}^2}S\right)d\hat{x}d\hat{t} = \\ &-\int R \cdot S\sum_{i=1}^{N-1}\left(X_i\frac{\partial C_i}{\partial\hat{t}} + \frac{\partial X_i}{\partial\hat{x}}C_i - \frac{1}{\mathrm{Pe}}\frac{\partial^2 X_i}{\partial\hat{x}^2}C_i\right)d\hat{x}d\hat{t}\end{aligned} \tag{8}$$

It is worth to noting some important features of Eq. (8). First, given the separated form of the solution (Eq. 5), the time derivative operates only on S, while the derivatives with respect of space coordinate x act only on R. Second, the right-hand side of Eq. (8) is known since it involves the approximated solution θ^{n-1} which is known at the enrichment step n.

The integration with respect of $\hat{t}$ can be now performed. This is made possible once again because independent variables $\hat{x}$ and $\hat{t}$ appear in a separated fashion (Eqs. 4 and 5), and because at the first step of the alternating strategy function S is known. Such an integration leads to:

$$\int R\left(s_1 \cdot R + s_2 \cdot \frac{\partial R}{\partial\hat{x}} - s_2 \cdot \frac{1}{\mathrm{Pe}}\frac{\partial^2 R}{\partial\hat{x}^2}\right)d\hat{x} = -\int R\sum_{i=1}^{N-1}\left(s_3^i \cdot X_i + s_4^i \cdot \frac{\partial X_i}{\partial\hat{x}} - s_4^i \cdot \frac{1}{\mathrm{Pe}}\frac{\partial^2 X_i}{\partial\hat{x}^2}\right)d\hat{x} \tag{9}$$

Or going back to the strong formulation:

$$s_1 \cdot R + s_2 \cdot \frac{\partial R}{\partial \hat{x}} - s_2 \cdot \frac{1}{\mathrm{Pe}} \frac{\partial^2 R}{\partial \hat{x}^2} = -\sum_{i=1}^{N-1} \left(s_3^i \cdot X_i + s_4^i \cdot \frac{\partial X_i}{\partial \hat{x}} - s_4^i \cdot \frac{1}{\mathrm{Pe}} \frac{\partial^2 X_i}{\partial \hat{x}^2} \right) \tag{10}$$

where

$$s_1 = \int_0^1 S \frac{dS}{d\hat{t}} d\hat{t} \quad s_2 = \int_0^1 S^2 d\hat{t} \quad s_3^i = \int_0^1 S \frac{dC_i}{d\hat{t}} d\hat{t} \quad s_4^i = \int_0^1 S C_i d\hat{t} \tag{11}$$

Equation (10) represents a 1D boundary value problem that can be solved for *R* using any suitable numerical method (e.g. finite differences). Once *R* has been computed, the second step of the alternating strategy can be performed, namely:

- Second step - compute $S(\hat{t})$ from the last evaluation of $R(\hat{x})$:

This step proceeds in a similar way as the first one: weak formulation (9) is used again, however now integration over $\hat{x}$ is performed since *R* is known from step one. Such an integration leads to the following initial value problem:

$$r_1 \cdot \frac{\partial S}{\partial \hat{t}} + r_3 \cdot S - r_2 \cdot \frac{1}{\mathrm{Pe}} S = -\sum_{i=1}^{N-1} \left(r_4^i \cdot \frac{\partial C_i}{\partial \hat{t}} + r_6^i \cdot C_i - r_5^i \cdot \frac{1}{\mathrm{Pe}} C_i \right) \tag{12}$$

where

$$r_1 = \int_0^1 R^2 d\hat{x} \quad r_2 = \int_0^1 R \frac{d^2 R}{d\hat{x}^2} d\hat{x} \quad r_3 = \int_0^1 R \frac{dR}{d\hat{x}} d\hat{x} \quad r_4^i = \int_0^1 R X_i d\hat{x} \quad r_5^i = \int_0^1 R \frac{d^2 R}{d\hat{x}^2} d\hat{x} \quad r_6^i = \int_0^1 R \frac{dR}{d\hat{x}} d\hat{x} \tag{13}$$

The initial value problem (12) can be then solved using a standard integration scheme such as Runge-Kutta method.

Step 1 and step 2 are iterated alternately until *R* and *S* converges to the desired functions X_n and C_n. The convergence of the alternating strategy is assessed comparing the solution found for two subsequent iterations [6]:

$$\left\| R^{k-1}(\hat{x}) S^{k-1}(\hat{t}) - R^k(\hat{x}) S^k(\hat{t}) \right\| < \varepsilon \tag{14}$$

Where index *k* identifies the number of iterations of the alternating strategy, while ε is a prescribed tolerance. In the present work L^2 norm was used for Eq. (14).

The complete PGD algorithm for the computation of the separated solution (3) it is here reported:

```
Start n = 1
    Set k = 1
        Compute R form S (Eq. 10)
        Compute S from last R (Eq. 12)
        if ||R^{k-1} S^{k-1} − R^k S^k|| < ε (Eq. 14)
            set R^k → X_n; S^k → C_n;
            return to start; n ← n +1;
        else
    k ← k+1
end
```

The enrichment procedure is stopped when the solution in the separate form (4) satisfies Eq. (2) within a prescribed error $E(n)$. Here the following stopping criteria [6] for the enrichment procedure is adopted:

$$\left\| \frac{X_n(\hat{x})C_n(\hat{t})}{X_1(\hat{x})C_1(\hat{t})} \right\| < E(n) \tag{15}$$

2.1.1. Results

The sensible TES system for the district heating network of Turin (Italy) studied in [14] was considered to test the performance of PGD. The system is 30 m high and has a diameter of 3.5 m. the operating temperature range is 120 – 65°C (T_{max} – T_{min}) and it can provide up to 100 MW_{th} for about 1 hour during discharge. Figure 3 depicts the time evolution of dimensionless temperature θ in the storage tank predicted with the PGD method. Storage tank was considered fully charged at t = 0 while θ = 0 was enforced as boundary condition at $\hat{x} = 0$ (inlet of the tank). An outflow boundary condition was prescribed at $\hat{x} = 1$. In Fig. 3 the solution predicted using PGD is compared with the solution obtained with traditional CFD finite-volume method. The latter was validated in [14]. It is clear that the number of terms N included in the separate form (3) drastically affects the accuracy of the solution. 80 terms make the PGD solution identical to the one obtained with traditional CFD. The accuracy of the PGD solution is further investigated in Fig. 4. The latter presents the error estimation $E(N)$ as a function of N according to Eq. (15). Error is estimated to be ~10^{-2} for N = 20, while it drops to ~10^{-5} for a separated solution with 80 terms included.

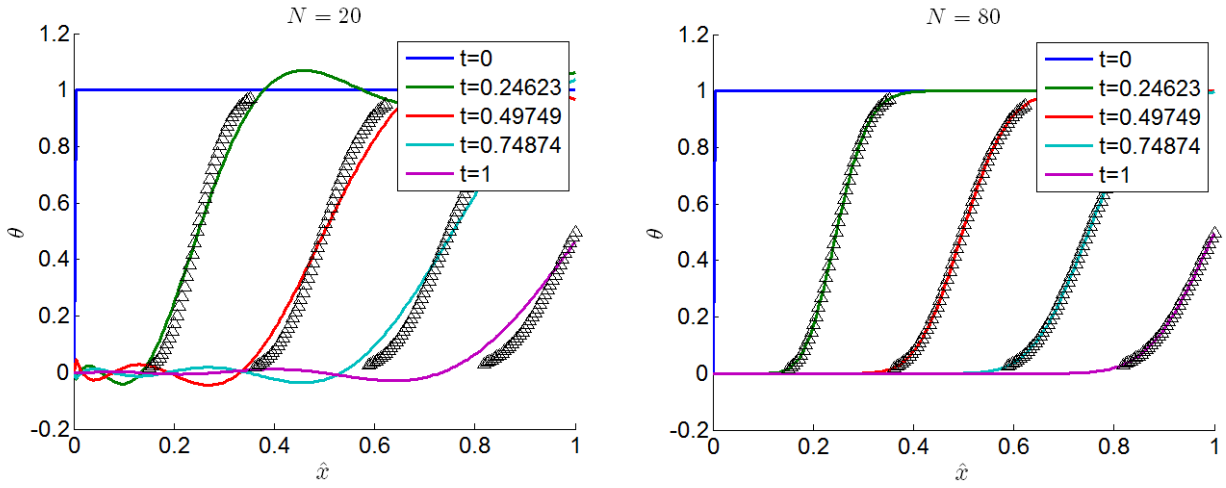

Fig. 3. PGD solution with 20 terms (left) and 80 terms (right); (Δ) CFD solution.

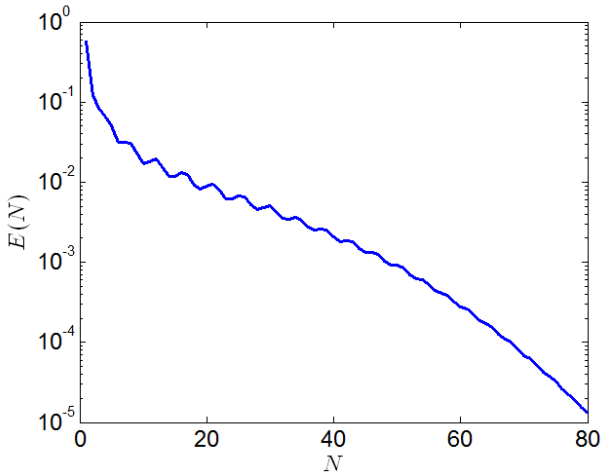

Fig. 4. Error estimation as a function of number of terms N in the solution.

Normalized functions X_i and C_i obtained through by the PGD are illustrated in Fig. 5 for $i = 1,\ldots,4$. In can be seen that the functions X_1, C_1 are constants in their corresponding domain since they are used to enforce boundary and initial conditions according to the procedure illustrated in [15]. Overall, the first terms in the separated solution account for the main dynamical features of the TES systems, while the higher-order X_i, C_i account for small perturbation of the overall dynamics. This can be also seen in Fig. 3. Twenty terms ($N = 20$) were sufficient to capture the main feature of the solution, however it was necessary to add other 60 terms ($N = 80$) to carefully predict the temperature time evolution in the sensible storage tank.

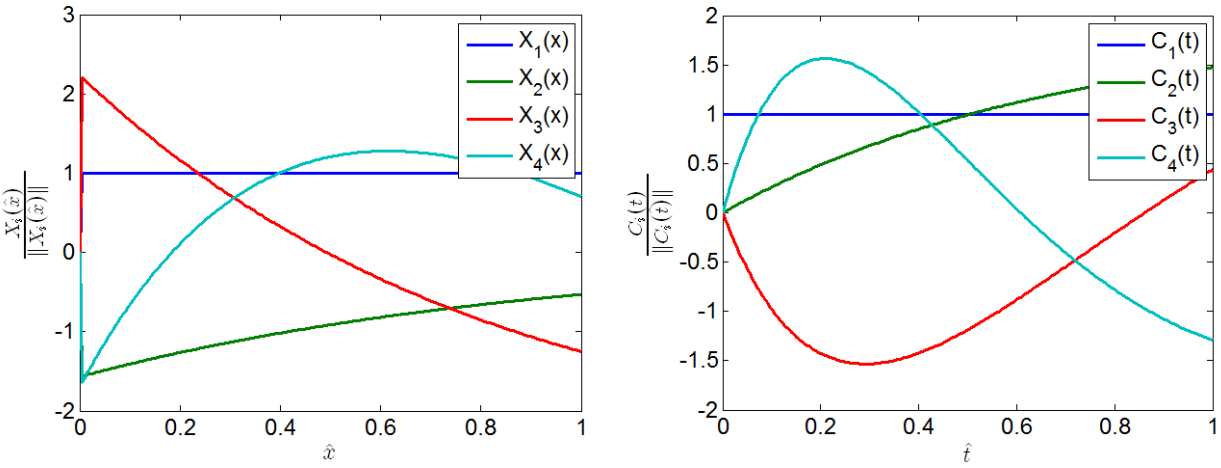

Fig. 5. Normalized PGD functions for i = 1,…,4.

2.2. PGD as generalized solver

In this section a PGD model of the TES system is developed to *a-priori* account in the solution the effect of possible design parameters or operation parameters. To this aim, energy equation (2) is here revisited with a different prospective. In such dimensionless equation the design/operation parameters are condensed in the Peclet number ($\mathrm{Pe} = uH/\alpha$). Thermal α diffusivity represents a design parameter, in fact a different choice of the storage medium would imply a variation in the Pe number. In a similar manner a change of fluid flow velocity u in the tank involves a modification of the Pe number. This latter case represents a variation of the operating condition of the sensible storage system. Indeed, the rate of thermal energy retrieved from a thermocline TES, such as the one here considered, is adjusted by controlling the mass flow rate, and therefore the velocity, of the liquid storage medium in the tank. A generalized model which *a-priori* includes a *spectrum* of Pe numbers was developed considering Pe number as an additional "dimension" of the problem and by introducing it in the separated solution:

$$\theta(\hat{x},\hat{t},\mathrm{Pe}) = \sum_{i=1}^{N} X_i(\hat{x}) C_i(\hat{t}) P_i(\mathrm{Pe}) \tag{16}$$

where now the extra set of functions P_i(Pe) appear on right-hand side to account for the extra dimension included of the problem. The calculation of X_i, C_i and P_i proceeds similarly to what illustrated in section 2.1. Namely, at each enrichment step n the the functions X_i, C_i and P_i are computed one by one through an alternating strategy. At the n-th enrichment step the solution is

$$\theta^n = \theta^{n-1} + R(\hat{x}) S(\hat{t}) U(\mathrm{Pe}) \tag{17}$$

where R, S and U are the approximations of functions X_i, C_i and P_i, respectively. The alternating strategy prescribes three steps:

- First step - compute $R(\hat{x})$ from $S(\hat{t})$ and $U(\mathrm{Pe})$

- Second step - compute $S(\hat{t})$ from $R(\hat{x})$ (computed at step 1) and $U(\mathrm{Pe})$
- Third step - compute $U(\mathrm{Pe})$ from $R(\hat{x})$(computed at step 1) and $S(\hat{t})$ (computed at step 2)

At each step the weighted residual form

$$\int R \cdot S \cdot U \left(\frac{\partial \theta}{\partial \hat{t}} + \frac{\partial \theta}{\partial \hat{x}} - \frac{1}{\mathrm{Pe}} \frac{\partial^2 \theta}{\partial \hat{x}^2} \right) d\hat{x} d\hat{t} d\mathrm{Pe} = 0 \tag{18}$$

is considered and Eq. (17) is substituted into it. Then, integration over two of the three dimensions is performed taking advantage of the separate form of the solution. Such an integration procedure is similar to the one is illustrated in Sect. 2.1 by Eq. (9). The key difference here consists in the fact that $\theta(\hat{x}, \hat{t}, \mathrm{Pe})$ now involves three dimensions, *x*, *t*, and Pe. Thus, at each of the three steps of the alternating strategy the integration is carried out over the two dimensions corresponding to the known functions. For example, at the first step integration over $\hat{t}$ and Pe is performed since *R* is calculated starting from *S* and *U*. Such a procedure leads to a boundary value problem (Eq. 19), a intial value problem (Eq. 20) and an algebraic problem (Eq. 21):

$$s_1 \cdot u_1 \cdot R + s_2 \cdot u_1 \cdot \frac{\partial R}{\partial \hat{x}} - s_2 \cdot u_2 \cdot \frac{\partial^2 R}{\partial \hat{x}^2} = -\sum_{i=1}^{N-1} \left(s_3^i \cdot u_3^i \cdot X_i + s_4^i \cdot u_3^i \cdot \frac{\partial X_i}{\partial \hat{x}} - s_4^i \cdot u_4^i \cdot \frac{\partial^2 X_i}{\partial \hat{x}^2} \right) \tag{19}$$

$$r_1 \cdot u_1 \cdot \frac{\partial S}{\partial \hat{t}} + r_3 \cdot u_1 \cdot S - r_2 \cdot u_2 \cdot S = -\sum_{i=1}^{N-1} \left(r_4^i \cdot u_3^i \cdot \frac{\partial C_i}{\partial \hat{t}} + r_6^i \cdot u_3^i \cdot C_i - r_5^i \cdot u_4^i \cdot C_i \right) \tag{20}$$

$$r_1 \cdot s_1 \cdot U + r_3 \cdot s_2 \cdot U - \frac{1}{\mathrm{Pe}} \cdot r_2 \cdot s_2 \cdot U = -\sum_{i=1}^{N-1} \left(r_4^i \cdot s_3^i \cdot P_i + r_6^i \cdot s_4^i \cdot P_i - \frac{1}{\mathrm{Pe}} \cdot r_5^i \cdot s_4^i \cdot P_i \right) \tag{21}$$

where

$$r_1 = \int_0^1 R^2 d\hat{x} \quad r_2 = \int_0^1 R \frac{d^2 R}{d\hat{x}^2} d\hat{x} \quad r_3 = \int_0^1 R \frac{dR}{d\hat{x}} d\hat{x} \quad r_4^i = \int_0^1 R X_i d\hat{x} \quad r_5^i = \int_0^1 R \frac{d^2 R}{d\hat{x}^2} d\hat{x} \quad r_6^i = \int_0^1 R \frac{dR}{d\hat{x}} d\hat{x} \tag{22}$$

$$s_1 = \int_0^1 S \frac{dS}{d\hat{t}} d\hat{t} \quad s_2 = \int_0^1 S^2 d\hat{t} \quad s_3^i = \int_0^1 S \frac{dC_i}{d\hat{t}} d\hat{t} \quad s_4^i = \int_0^1 S C_i d\hat{t} \tag{23}$$

$$u_1 = \int_0^1 U^2 d\mathrm{Pe} \quad u_2 = \int_0^1 \frac{1}{\mathrm{Pe}} U^2 d\mathrm{Pe} \quad u_3^i = \int_0^1 U P_i d\mathrm{Pe} \quad u_4^i = \int_0^1 \frac{1}{\mathrm{Pe}} U P_i d\mathrm{Pe} \tag{24}$$

Equations (19-21) can be solved to compute *R*, *S*, and *U*. This calculation is iterated until *R*, *S*, and *U* converge to the desired functions X_n, C_n, P_n. The convergence criteria for the alternating strategy and for the enrichment procedure are the following:

$$\left\| R^{k-1}(\hat{x}) S^{k-1}(\hat{t}) U^{k-1}(\mathrm{Pe}) - R^k(\hat{x}) S^k(\hat{t}) U^{k-1}(\mathrm{Pe}) \right\| < \varepsilon \tag{22}$$

$$\left\| \frac{X_n(\hat{x}) C_n(\hat{t}) P_n(\mathrm{Pe})}{X_1(\hat{x}) C_1(\hat{t}) P_1(\mathrm{Pe})} \right\| < E(n) \tag{23}$$

2.2.1. Results

The generalized solver described in the previous section is here employed to model the sensible TES system for 100 different Pe numbers in the range 2 – 20. This means that 100 scenarios corresponding to different design/operating conditions. Once the separated solution (16) has been

calculated, each single case can be obtained as a simple *post-processing* of the generalized solution. For example, the cases corresponding to Pe = 200 and Pe = 20 are obtained as follow:

$$\theta(\hat{x},\hat{t},\mathrm{Pe}=200)=\sum_{i=1}^{N}X_i(\hat{x})C_i(\hat{t})P_i(\mathrm{Pe}=200) \tag{24}$$

$$\theta(\hat{x},\hat{t},\mathrm{Pe}=20)=\sum_{i=1}^{N}X_i(\hat{x})C_i(\hat{t})P_i(\mathrm{Pe}=20) \tag{25}$$

That is, the generalized solution $\theta(\hat{x},\hat{t},\mathrm{Pe})$ is evaluated for the desired values of Pe number. This computation is at cost zero: no calculation are necessary because a *generalized solution* has been found since the beginning through the PGD solver. This is a key advantage of PGD that makes it an interesting technique for design analyses or optimization. Being the parameters/design variables included in the generalized solution, their optimal values according to a specified target (e.g. objective function) becomes a post-processing operation on the generalized solution which permits to avoid computational intensive optimization tasks. Figure 6 illustrates the two solutions mentioned above. A larger Pe number indicates a stronger advection contribution compared with the diffusive term (conduction). Thus, a sharper thermocline appears, as shown in the left plot of Fig. 6.

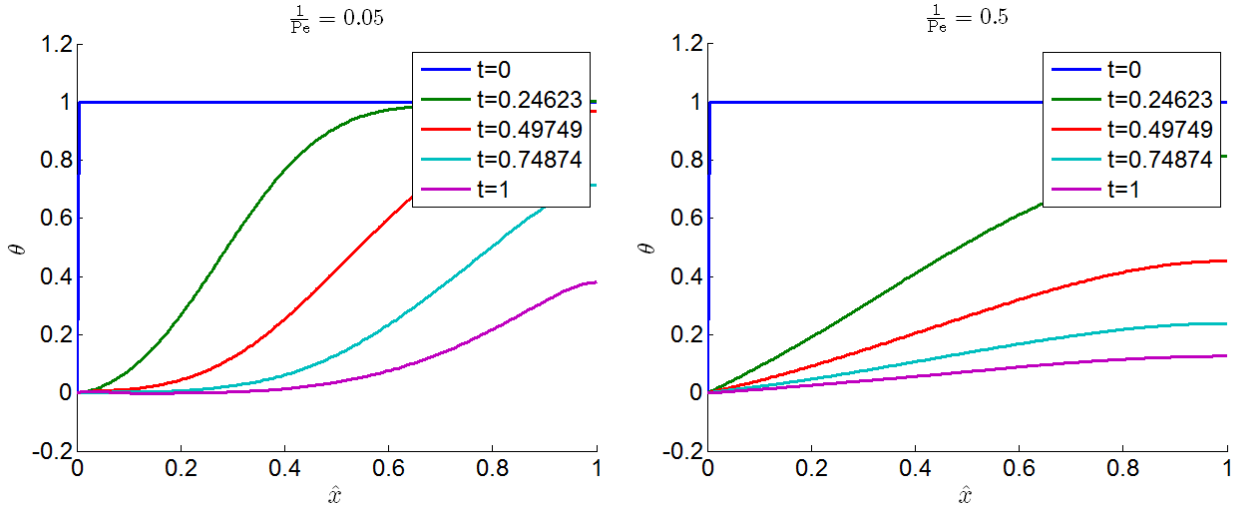

Fig. 6. PGD solutions for Pe = 200 (left) and Pe = 20 (right).

The generalized solution (16) involves three kind of PGD functions. The first four for each kind are shown in Fig. 7. Finally, the error estimation *E(N)* as a function of *N* according to Eq. (23) is presented in Fig. 7d. An important feature can be noted; as the number of dimensions of the problem increases, a larger number *N* of terms is necessary to achieve an accurate generalized solution. Furthermore, the rate of convergence is slower. An improvement of convergence rate and accuracy is current under investigation by the author together with his colleagues.

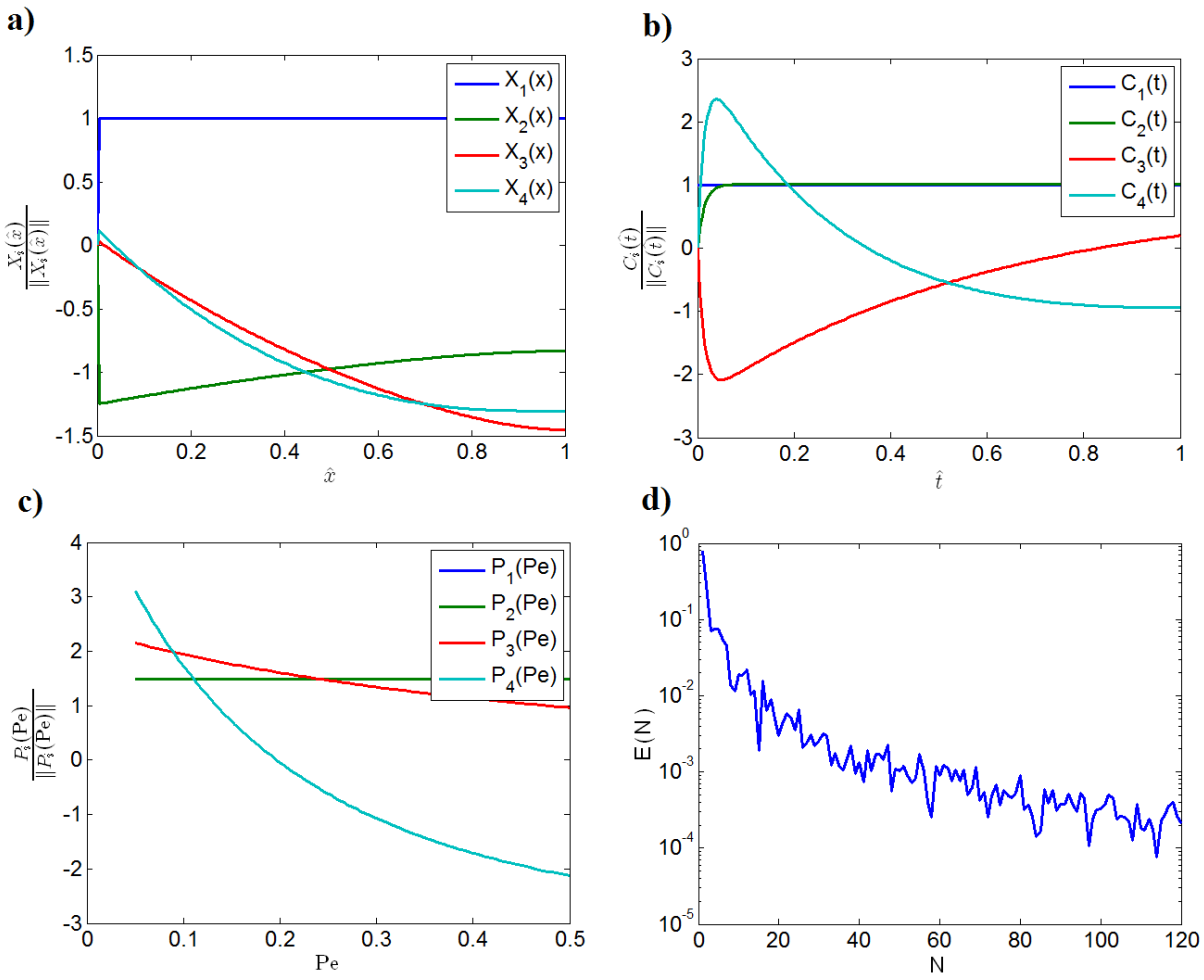

Fig. 7. a), b) and c) Normalized PGD functions for I = 1,…,4 (Eq. 16); d) Error estimation as a function of number of terms N in the solution (Eq. 23).

3. Conclusions

In this work we considered the transient behaviour of a sensible thermal energy storage system by using the proper generalized decomposition (PGD) method. This proceeds by enriching in sequence a solution in the separated form. That is, the solution consists in a sum of products of function of only one independent variable (e.g. *x* and *t*). This leads to separated one-dimensional models that can be solved numerical with a reduced computational effort.

We also showed the PGD as a generalized solver for including *a-priori* in the solution design/operating parameters. Specifically, the model for the thermal storage system was solved considering 100 different values of Pe number. Each particular solution for a fixed Pe number was then found through a simple post-processing of the generalized solution. These features of the PGD method makes it an effective technique to perform optimization and sensitivity analyses of energy systems. This work represents a first step toward this goal.

Nomenclature

C_i	PGD function [ ]
c_p	specific heat [J/kg K]
E	error estimation [ ]
k	thermal conductivity [W/m K]

Pe	Peclet number [ ]
P_i	PGD function [ ]
T	temperature [K]
t	time [s]
u	velocity [m/s]
X_i	PGD function [ ]
x	coordinate [m]
Θ	dimensionless temperature [ ]
ρ	density [kg/m^3]

References

[1] Sciacovelli A., Verda V., Borchiellini R. Numerical Design of Thermal Systems. Torino, ITA: Clut, 2013.

[2] Sciacovelli A., Verda V., Sciubba E. Entropy generation analysis as a design tool – A review. Renewable and Sustainable Energy Reviews 2015; 43:1167-181.

[3] Al-abidi A a., Bin Mat S, Sopian K, Sulaiman MY, Mohammed AT. CFD applications for latent heat thermal energy storage: a review. Renew Sustain Energy Rev 2013;20:353–63.

[4] Garcia-Martinez J., Wang Z.L., Nanotechnology for the Energy Challenge. Hoboken, USA: John Wiley & Sons, Inc.; 2009.

[5] Rao S., Engineering Optimization – Theory and Practice. Hoboken, USA: John Wiley & Sons, Inc.; 2009.

[6] Chinesta F., Ammar A., Cueto E. Recent Advances and New Challenges in the Use of the Proper Generalized Decomposition for Solving Multidimensional Models. Arch Comput Methods Eng 2010; 17: 327–350.

[7] Chinesta F., Ladeveze P., Cueto E. A Short Review on Model Order Reduction Based on Proper Generalized Decomposition. Arch Comput Methods Eng 2011; 18:395–404.

[8] Ifrah G., The universal history of computing. Hoboken, USA: John Wiley & Sons, Inc.; 2001.

[9] Schilders W.H.A A. van der Vorst H.A., Rommes J. Model Order Reduction: Theory, Research Aspects and Applications. Berlin: Springer-Verlag; 2008.

[10] Buljak V., Inverse Analyses with Model Reduction. Berlin: Springer-Verlag; 2012.

[11] Han Y.M., Wang R.Z., Dai Y.J. Thermal stratification within the water tank. Renewable and Sustainable Energy Reviews 2009; 13: 1014–026.

[12] Chinesta F., Ammar A., Leygue A., Keunings R. An overview of the proper generalized decomposition with applications in computational rheology. J. Non-Newtonian Fluid Mech. 2011; 166:578–592.

[13] Quarteroni A., Numerical Modeling for Differential Problems. Springer-Verlag Italia, Milan 2009.

[14] Verda V., Colella F. Primary energy savings through thermal storage in district heating. Energy 2011;36: 4278-286.

[15] Gonzalez D., Ammar A., Chinesta F., Cueto E. Recent advances on the use of separated representations. Int. J. Numer. Meth. Engng 2010; 81:637–659.